Nuclear Instruments and Methods in Physics Research A 365 (1995) 572–575

ELSEVIER

NUCLEAR INSTRUMENTS & METHODS IN PHYSICS RESEARCH Section A

Letter to the Editor

Potential distribution within semiconductor detectors using coplanar electrodes

Zhong He*

Nuclear Engineering Department, The University of Michigan, Ann Arbor, MI 48109-2104, USA

Received 13 March 1995

Abstract

The analytical form of the potential distribution within room-temperature of semiconductor detectors, which use periodic parallel strip electrodes, is presented. The results can be extended to account for the case of 2-D segmented electrode arrays. The induced charge on corresponding electrodes and implications of this analysis are discussed. This could help the design of detectors that have significant charge trapping problems, and to achieve good position sensitivity by making use of the trapping characteristics. Some calculated results have been compared with that obtained using finite element analysis by other groups and the consistency is demonstrated.

Semiconductors having high atomic numbers and wide band-gaps have long been under development as potential room-temperature γ-ray detectors. Among those, HgI_2 [1,2], CdTe [3] and CdZnTe [4] detectors have attracted most of the attention. Although these semiconductors have been successfully employed in various applications, the widespread use of these devices has been hindered by their charge trapping [4] and polarization [5] problems. Continuing effort has been given to improve the characteristics of the materials [4,6], but the energy resolution achieved using conventional planar electrodes is still far worse than what people could expect. Good energy resolutions were obtained by applying different signal processing techniques [7,8] at the expense of complexity of the electronic system or severe loss of detection efficiency. Recently, significant progress has been reported by Luke [9,10] which could lead to a major change in the design of readout systems of room-temperature semiconductor detectors. Luke's method is based on the principle of Frisch grids [11] commonly employed in gas ion chambers, but uses parallel coplanar strip electrodes. The strips are connected in an alternate manner to give two sets of inter-digital grid electrodes. By reading the difference signal between these two sets of electrodes, pulses induced by one type (electrons or holes) of charge carriers can be obtained. For commonly used semiconductor detectors, signals from electrons produced by γ-ray interaction can be picked out so that the hole trapping problem can be eliminated. Following Luke's work, Barrett et al. [12] have suggested that the single-polarity charge sensing can also be approached by segmenting one side of conventional planar electrodes into small elements to form a 2-D electrode array, and to read signals individually from each of the square electrode pixels.

This paper presents the analytical form of the field distribution for a more generalized configuration of coplanar strip electrodes, obtained using the standard method of separation of variables [13]. The results can be easily extended for 2-D segmented electrode arrays [12,2]. This analysis could help to have a better insight into the configuration of the electric field within the detector and provides a simpler method for calculating both the operating field and weighting field potentials. Therefore, the induced charge on corresponding electrodes as a function of time can be easily estimated.

The basic structure of coplanar strip electrodes used by Luke [9] is shown schematically in an end-on view in Fig. 1. For simplicity, we ignore the variations along the direction of strips (Z axis). The solution of the potential distribution $\varphi(x, y)$ within the semiconductor detector is obtained under the following assumptions:

1) Within the detector volume $\varphi(x, y)$ satisfies the Laplace equation (it is only an approximation when space charge is not significant):

$$\nabla^2\varphi(x, y) = 0\,. \tag{1}$$

2) The field is symmetric relative to a YZ plane, we

* Tel. +1 313 764 5285, e-mail hezhong@engin.umich.edu.

SSDI 0168-9002(95)00676-1

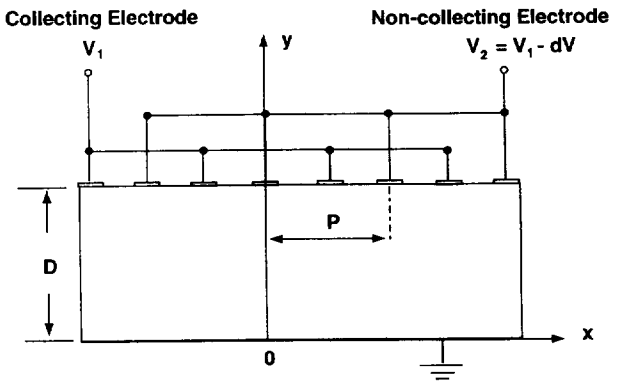

Fig. 1. End-on view of the coplanar strip electrodes.

let this plane to be $x = 0$ in Fig. 1. This gives: $\partial\varphi(x, y)/\partial x = 0$ at $x = 0$.

3) The period along x axis is P.

4) $\varphi(x, y) = 0$ at $y = 0$.

5) $\varphi(x, y) = \varphi_D(x)$ at $y = D$.

Since it is periodic along the x axis, $\varphi(x, y)$ is obtained only within one period ($0 \le x \le P$).

From the standard method of separation of variables ([13] p. 68), it can be assumed that the potential $\varphi(x, y)$ can be represented by a product of two functions, one for each coordinate:

$$\varphi(x, y) = X(x)Y(y) . \tag{2}$$

It can be obtained from Eqs. (1) and (2) that

$$\frac{1}{X}\frac{d^2X}{dx^2} = -\alpha^2 , \quad \frac{1}{Y}\frac{d^2Y}{dy^2} = \alpha^2 , \tag{3}$$

where α is a constant. Since both X and Y are real functions, α^2 has to be real. It can be shown that solutions with negative α^2 values can not satisfy boundary conditions, so that $\alpha^2 \ge 0$. This makes X and Y have the following forms:

$$X(x) = a\,e^{i\alpha x} + b\,e^{-i\alpha x} , \tag{4}$$

$$Y(y) = c\,e^{\alpha y} + d\,e^{-\alpha y} , \tag{5}$$

where a, b, c and d are constants. Assumptions (2), (3) and (4) give:

$$a = b , \quad c = -d , \quad \alpha = 2\pi n/P ,$$
$$n = -\infty, \cdots -1, 0, +1, \cdots +\infty .$$

From these conditions, one can see that $X(x)Y(y)$ with negative n is the same as that obtained from the positive, apart from an unimportant constant. Therefore, the summation can be done only for positive n values. It should be noticed that when $n = 0$, which corresponds to the case of $\alpha = 0$, the solution of $Y(y)$ is of the form cy (satisfying assumption (4)). As a result, the potential $\varphi(x, y)$ can thus be built up from the product of solutions:

$$\varphi(x, y) = c_0 y + \sum_{n=1}^{\infty} c_n \cos\frac{2\pi n}{P} x \sinh\frac{2\pi n}{P} y , \tag{6}$$

where c_0 and c_n are constant. From Eq. (6), assumption (5) and the orthogonal properties of cosine functions, $\varphi(x, y)$ is obtained as:

$$\varphi(x, y) = a_0\left(\frac{y}{D}\right) + \sum_{n=1}^{\infty} a_n \cos\frac{2\pi n}{P} x \cdot \left(\frac{\sinh\frac{2\pi n}{P} y}{\sinh\frac{2\pi n}{P} D}\right), \tag{7}$$

$$a_0 = \frac{1}{P}\int_0^P \varphi_D(x)\,dx , \quad a_n = \frac{2}{P}\int_0^P \varphi_D(x)\cos\frac{2\pi n}{P} x\,dx .$$

In practice, the spatial period P usually satisfies the condition $P \ll D$, and Eq. (7) approaches:

$$\varphi(x, y) \approx a_0\left(\frac{y}{D}\right) + \sum_{n=1}^{\infty} a_n \cos\frac{2\pi n}{P} x \cdot \exp\left(-2\pi n\frac{D-y}{P}\right) . \tag{8}$$

As one can see, a_0 and a_n are Fourier-transform coefficients of $\varphi_D(x)$. The potential $\varphi(x, y)$ is then just the inverse Fourier-transform having each a_n multiplied by an exponential factor, with the exception of a_0 multiplied by a linear term of y. At any particular y, the first term in Eq. (8) accounts for the average of $\varphi(x, y)$ over x, and the second term gives the deviation from the average value. It is evident that the deviation from the average at any y is modulated mainly by the exponential factor corresponding to $n = 1$. At $y = D - P/2$ and $y = D - P$, the amplitudes of deviations are reduced to about $\exp(-\pi)$ and $\exp(-2\pi)$ compared to that at $y = D$, which are about 4.3% and 0.2% respectively. This is consistent with the results obtained using finite element analysis [9,10].

For numerical calculations, the discrete form of Eq. (7) can be simplified by letting $P = 1$, $x_i = (i-1)/N$, $i = 1, 2, \cdots N$ and $dx = 1/N$. The Fourier coefficients a_n need only be calculated up to $n = N/2$, which corresponds to the Nyquist critical frequency. Eq. (7) can then be written as:

$$\varphi(x_i, y_j) = a_0\left(\frac{y_j}{D}\right) + \sum_{n=1}^{N/2} a_n \cos\frac{2\pi n(i-1)}{N} \cdot \frac{\sinh(2\pi n y_j)}{\sinh(2\pi n D)} , \tag{9}$$

$$a_0 = \frac{1}{N}\sum_{i=1}^{N} \varphi_D(x_i) , \quad a_n = \frac{2}{N}\sum_{i=1}^{N} \varphi_D(x_i)\cos\frac{2\pi n(i-1)}{N} .$$

Both y_j and D are in units of P. Fig. 2 shows the operating potential distribution, when space charge is

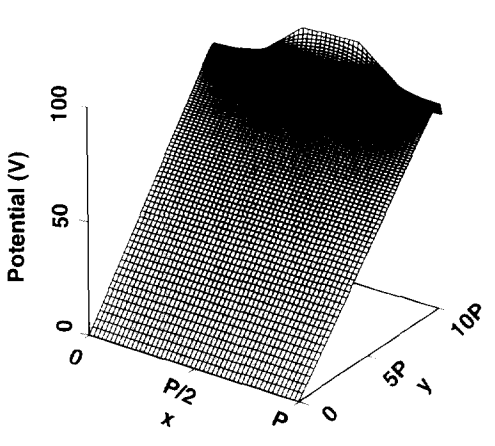

Fig. 2. Operating potential when $V_1 = 100$ V, $V_2 = 80$ V, $D = 10P$, electrodes and gaps have the same width.

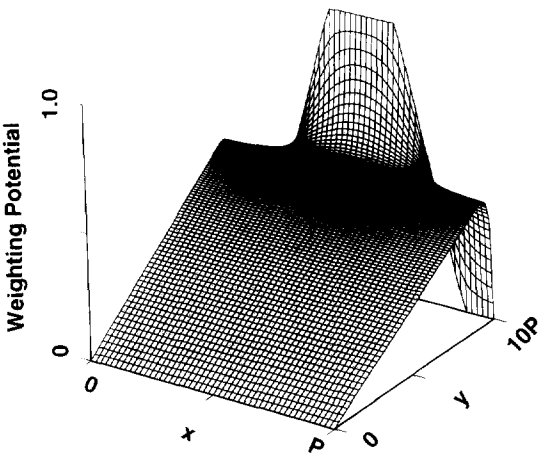

Fig. 3. Weighting potential distribution for the same configuration as in Fig. 2.

not significant, within a semiconductor detector calculated using Eq. (9) under the following conditions: strip electrodes and gaps between electrodes have the same width, the collecting electrodes are at 100 V and the non-collecting electrodes are at 80 V. The current i induced on an electrode due to the movement of a charge Q can be calculated using the Ramo–Shockley theorem [14,15]:

$$i = Q\boldsymbol{v} \cdot \boldsymbol{E}_w \,. \tag{10}$$

where $\boldsymbol{v}$ is the instantaneous velocity of charge Q, and $\boldsymbol{E}_w = -\nabla\varphi_w(x, y)$ is the weighting field which would exist at the position of Q under the following circumstances: the charge Q is removed, the selected electrode at unit potential and all other electrodes are grounded. The weighting potential corresponding to the above detector configuration was calculated using Eq. (9) and is shown in Fig. 3. The results are consistent with that of Luke [9,10] obtained using finite element analysis. The potential distribution between electrodes on the $y = D$ plane was approximated using linear interpolation.

The velocities of charge carriers generated by γ-ray interactions can be estimated using equations:

$$\boldsymbol{v}_e = \mu_e \boldsymbol{E}_{opt} \,, \quad \boldsymbol{v}_h = \mu_h \boldsymbol{E}_{opt} \,, \tag{11}$$

where μ_e and μ_h are mobilities of electrons and holes, and $\boldsymbol{E}_{opt} = -\nabla\varphi_{opt}(x, y)$ is the operating field. Charge trapping can be considered by:

$$Q_e = eN_0\, e^{-t/\tau_e} \,, \quad Q_h = eN_0\, e^{-t/\tau_h} \,. \tag{12}$$

where τ_e and τ_h are life-times of electrons and holes. The induced charge as a function of time may be calculated using Eqs. (9)–(12) and the results were consistent with Ref. [10] (Fig. 10).

Some implications of Eq. (7) are listed as follows:

1) The voltage difference between the collecting and non-collecting electrodes should be set so that the potential difference between the maximum along the field line passing through the centre of the non-collecting electrodes and that on the non-collecting electrodes is greater than the kinetic energy of the collecting charge carriers. This will ensure that the electric field can guide selected charge carriers onto the collecting electrodes.

2) The widths of collecting and non-collecting strip electrodes have to be the same. This makes that the weighting fields of the two electrodes have identical linear terms, so that charge carriers within that region induced the same amount of charge on both electrodes. By reading out the difference between the two electrodes, only the signal induced by charge carriers moving within the vicinity ($D - P < y < D$) of coplanar electrodes can be picked out.

3) The unipolar charge sensing technique could also be approached by reading out signals from strip electrodes individually. This can be understood from the weighting field distribution of the selected electrode. An example is shown in Fig. 4 which assumes electrodes and gaps have the same width. In this case, the space period P in Eq. (7) was chosen to be 20 times the pitch of the electrodes. As one can see, the average value a_0 of $\varphi_D(x)$ of the corresponding weighting field approaches zero as more electrodes are included. Therefore, the linear part of the weighting field can be very close to zero, and the weighting potential rises to 1 rapidly at the vicinity of the selected electrode. In practice, the minimum space period of electrodes is limited by the condition that the charge carriers are mainly collected by a single electrode.

4) Two dimensional segmented electrode arrays have been used by many groups [1,2,4] for γ-ray

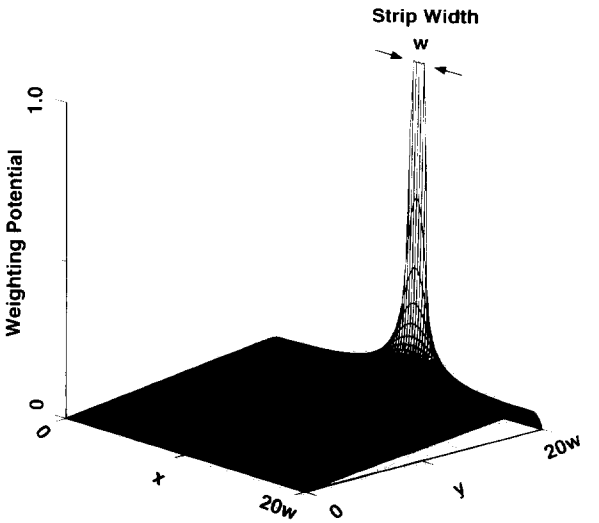

Fig. 4. Weighting potential distribution of a single strip electrode.

imaging applications. Barrett et al. [12] have suggested very recently that single polarity charge sensing can be approached by properly choosing the pixel size of two dimensional segmented electrode arrays, and by reading out signals from individual pixels. They have demonstrated it both in theory and experiments. One thing in common on these detectors is that all pixels of the electrode array were biased at the same potential. The field distribution in these semiconductor detectors can be assumed to be more general in order to account for cases where electrode elements are connected to slightly different potentials, such as the example shown in Fig. 5. It is easy to show that Eq. (7) can be extended to this three dimensional case, where $\varphi(x, y, z)$ has symmetry and is periodic both in x and y directions. Similar to the case of individual strip read

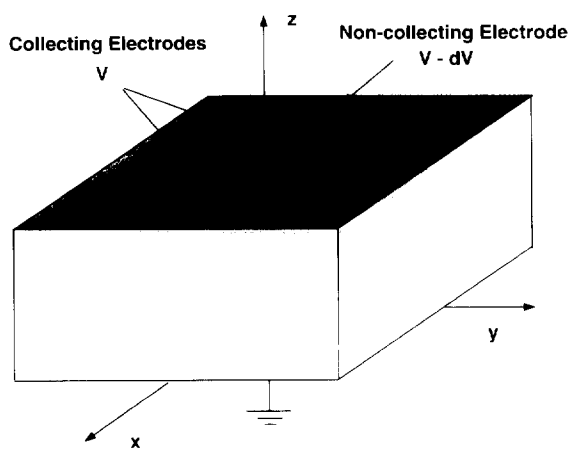

Fig. 5. Illustration of a detector with 2-D segmented electrode array.

out, the weighting potential of a selected pixel of collecting electrodes is very close to zero in the detector volume and rises rapidly to 1 while it approaches the pixel within a distance of one space period. It could be advantageous to bias the non-collecting electrode at a slightly lower potential to that of the collecting electrodes, in contrast to all electrodes biased at the same voltage: (1) Charge carriers could be guided by the electric field so that the gap effect could be improved. (2) The induced signal on the non-collecting electrode could be used to achieved position-sensing along the z axis, and to correct for electron trapping while electrons are collected by collecting electrodes.

Acknowledgements

This work would not be possible without the leadership of Prof. G.F. Knoll. The author thanks R.A. Rojeski and Prof. D.K. Wehe for their invaluable discussions. The work was supported by the Department of Energy under contract number DE-FG08-94NV11630.

References

[1] D. Ortendahl et al., IEEE Trans. Nucl. Sci. NS-29(1) (1982) 784.
[2] B.E. Patt et al., IEEE Trans. Nucl. Sci. NS-33(1) (1986) 523.
[3] E. Raiskin and J.F. Butler, IEEE Trans. Nucl. Sci. NS-35(1) (1988) 81.
[4] J.F. Butler et al., IEEE Trans. Nucl. Sci. NS-39(4) (1992) 605.
[5] V. Gerrish, Nucl. Instr. and Meth. A 322 (1992) 402.
[6] L.V.D. Berg, Nucl. Instr. and Meth. A 322 (1992) 453.
[7] L.T. Jones and P.B. Woollam, Nucl. Instr. and Meth. 124 (1975) 591.
[8] M. Richter and P. Siffert, Nucl. Instr. and Meth. A 322 (1992) 529.
[9] P.N. Luke, Appl. Phys. Lett. 65(22) (1994) 2884.
[10] P.N. Luke, Unipolar charge sensing with coplanar electrodes – application to semi-conductor detectors, Conf. Proc. of IEEE Nuclear Science Symp. and Medical Imaging Conf., Norfolk, Virginia, Oct. 30–Nov. 5, 1994.
[11] O. Frisch, British Atomic Energy Report BR-49, 1944.
[12] H.H. Barrett et al., Charge transport in arrays of semiconductor gamma-ray detectors, private communications, submitted to Phys. Rev. Lett. (1995).
[13] J.D. Jackson, Classical Electrodynamics, 2nd Ed. (Wiley, New York, 1975).
[14] S. Ramo, Proc. IRE 27(9) (1939) 584.
[15] W. Shockley, J. Appl. Phys. 9 (1938) 635.